Combined DTI and q-Space Analysis at High Angular Resolution of the Human Brain

Y. Assaf[1,2], O. Pasternak[3], P. J. Basser[4]

[1]Functional Brain Imaging Unit, Tel Aviv Sourasky Medical Center, Tel Aviv, Israel, [2]School of Chemistry, Tel Aviv University, Tel Aviv, Israel, [3]School of Computer Science, Tel Aviv University, Tel Aviv, Israel, [4]National Institute of Child Health and Human Development, The National Institutes of Health, Bethesda, MD, United States

Introduction

High b-value diffusion imaging complements diffusion tensor imaging (DTI) (1-2), in particular, providing specific information about water mobility in highly restricted compartments in white matter (2-4). This additional information has been found to be useful in detecting several white matter pathologies (2-3). If a significant portion of the signal observed at high b value originates from restricted motion of intra-axonal water (4), then it follows that it should be more sensitive than DTI to axonal morphology and could potentially improve the delineation of white matter tracts (5). We propose here an experimental framework that is clinically feasible for estimating parameters of a model of hindered and restricted diffusion in white matter (5) using high angular resolution diffusion weighted imaging (DWI) data obtained at both high and low b values.

Methods

Experiments were performed on healthy subjects scanned with a 3T MRI system (GE, Milwaukee, USA). High b value DWIs were acquired with the following parameters: TR/TE=2700/155ms, Δ/δ=53/47ms, G_{max}=3.4 Gauss/cm and 2 averages. Additional parameters were: 10 axial slices of 3 mm thick with no gap covering 30mm placed at below the top edge of the corpus callosum with FOV of 19cm, matrix size of 64x64 and resolution of 3x3x3 mm^3. The experiment was repeated for 169 diffusion gradient directions (at different b values according to the Table 1). For each b value the diffusion gradients were placed symmetrically and equally distributed over a sphere. The total acquisition time was 16 minutes.

Table 1

B value (s/mm^2)	No. of directions
0	1
714	6
1428	6
2285	12
3214	12
4286	16
5357	16
6429	20
7500	20
8571	30
10000	30

Data analysis was done according to a combined hindered and restricted model of diffusion described before (5). In general, the model combines contributions of hindered diffusion term arising from the extra-axonal spaces, and a restricted diffusion arising from the intraaxonal space. A diffusion tensor characterizes hindered diffusion, while the contribution from the restricted compartment is decomposed into signal arising from motion parallel and perpendicular motion to impermeable cylinders (modeling restricted diffusion in axons). Diffusion parallel to the fibers is free and modeled by the Stejskal-Tanner equation. Diffusion perpendicular to the fibers can be modeled using the theory of Neuman et al. (6) in which it is assumed that the diffusion gradients are constant, similar to the case in clinical scanners (i.e. $\Delta \sim \delta$). The general form of the model is given in Eq. [1] where f_h and f_r are the T_2-weighted population fraction of the hindered and restricted terms, $q_\perp$ and $q_{//}$ are the q vector components parallel and perpendicular to the fibers, Δ is the diffusion time, δ is the diffusion gradient duration, $\lambda_{//}$ and $\lambda_\perp$ are the diffusion tensor's eigenvalues parallel and perpendicular to the fibers, respectively, $D_{//}$ and $D_\perp$ are the parallel and perpendicular diffusion coefficients within the cylinders, R is the cylinder diameter, and τ is half the echo time. The noise floor is also estimated in the fitting procedure. The model can be expanded to include additional hindered and restricted compartments (Eq. [2]) allowing more than one orientation of fibers to be analyzed. The experimental data was fitted to the model using in-house Matlab© code that employs a non-linear least square routine (utilizing Levenberg-Marquardt minimization)

$$E(\mathbf{q},\Delta) = f_h \cdot e^{-4\pi^2\left(\Delta-\frac{\delta}{3}\right)\left(|\mathbf{q}_\perp|^2\lambda_\perp+|\mathbf{q}_{//}|^2\lambda_{//}\right)} + f_r \cdot e^{-4\pi^2|\mathbf{q}_{//}|^2\left(\Delta-\frac{\delta}{3}\right)D_{//}-\frac{4\pi^2R^4|\mathbf{q}_\perp|^2}{D_\perp\tau}\frac{7}{296}\left(2-\frac{99}{112}\frac{R^2}{D_\perp\tau}\right)} \quad [1]$$

$$E(\mathbf{q},\Delta) = \sum^{M} f_h^i \cdot E_h^i(\mathrm{q},\Delta) + \sum^{N} f_r^j \cdot E_r^j(\mathrm{q},\Delta) \quad [2]$$

Results

The signal decay at high b value shows poor SNR, yet seems to originate only from white matter which is placed perpendicular to the applied gradient direction (see Figure 1). The 169-image dataset was analyzed using the model on a pixel-by-pixel basis. Three parameters were kept fixed during the fitting procedure: The diffusion parallel and perpendicular with in the fibers ($D_{//}$ and $D_\perp$) as well as the axon diameter distribution, p(R). All other parameters were free and fitted simultaneously. In areas of homogeneous white matter the iso-displacement 3D plots of the hindered term and the restricted term provided similar orientations for fibers although the angular resolution of the restricted part seems to be better as it is shaped like a toothpick rather than an ellipsoid (see Figure 2). In areas of crossing fibers (in Figure 2 – marked by circle), the 3D iso-probability plots of the hindered part reveals a sphere which represents the powder average of all fiber directions in the pixel. By contrast the 3D iso-probability plots of the restricted part, which was fitted to a combination of 1 hindered and 2 restricted components, provided separation of the two diffusing components which seems to be aligned in reasonable orientations (Figure 2).

Figure 1

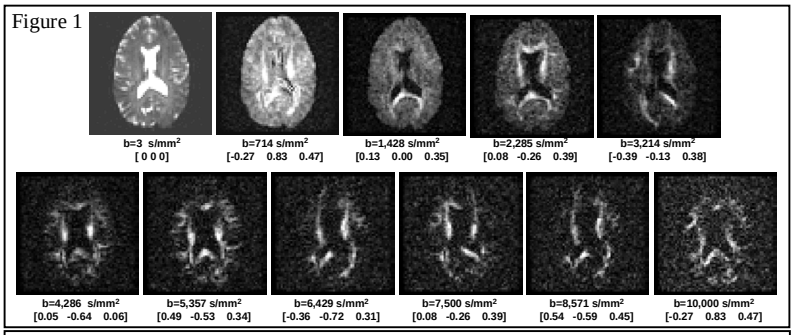

Figure 2

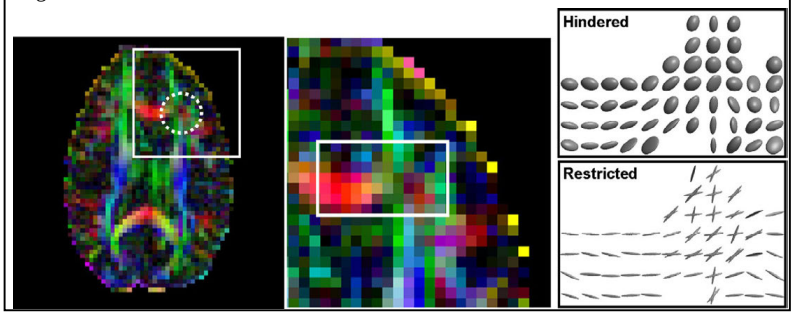

Discussion and Conclusions

The combined hindered and restricted model was able to distinguish between two orientations of fibers within the same pixel. This data was acquired within a reasonable time making this approach clinically feasible. The additional information it provides about fibers orientations and restricted diffusion may improve our ability to detect white matter pathologies. Nevertheless, a few questions remains unanswered: What is the relationship between the number of measured diffusion directions and the number of fiber orientations that can be extracted with reasonable accuracy? What is the certainty of the fibers orientations as extracted from the high b value data in view of the very poor SNR at the very high b value (see Figure 1)? The ability of the model to separate two (or more) fiber orientations may significantly improve fiber tracking methodologies, particularly in complicated neural pathways.

References

(1) Basser PJ. Magn Reson Med 2002;47:392. (2) Assaf Y, Ben-Bashat D, Chapman J et-al. Magn Reson Med 2002;47:115. (3) Assaf Y, Mayzel-Oreg O, Gigi A, et-al. J Neurol Sci 2002;203-204:235. (4) Assaf Y, Cohen Y. Magn Reson Med 2000;43:191. (5) Assaf Y, Basser PJ. Proc. Int. Soc. Magn. Reson. Med. 2003;11:588. (6) Neuman CH. J Chem Phys 1974;60:4508.